Refractive-index measurements of zinc germanium diphosphide at 300 and 77 K by use of a modified Michelson interferometer

Glen D. Gillen and Shekhar Guha

A method to determine the absolute refractive index of materials available in the shape of flat wafers with parallel sides by using interferometric techniques is presented. With this method, nondestructive, sample-specific measurements can be made. The method is tested by using silicon, germanium and zinc selenide, and measurements for both the ordinary and extraordinary axes of $ZnGeP_2$ for temperatures of 300 and 77 K are reported. © 2004 Optical Society of America

OCIS codes: 120.3180, 120.4290, 160.4760, 160.6000.

1. Introduction

It is important to know the absolute refractive indices of materials for most optical applications, especially for nonlinear light–matter interactions. Two methods for accurately measuring the refractive index of a material are the minimum deviation method[1,2] and ellipsometry.[3–5] The minimum deviation method is typically used for bulk materials, where some portion of the material is polished into the shape of a wedge or a prism. Ellipsometry is an accurate method for measuring the refractive index of thin films deposited on a substrate. Unfortunately, many infrared material samples grown as wafers with a thickness of a few millimeters or less do not easily fall into either of these two categories.

For the types of material that can be manufactured sufficiently thick for accurate wedge- or prism-shaped samples to be formed, other challenges arise. Although refractive-index measurements performed by the minimum deviation method are highly accurate, they do require the sacrifice of some portion of the material to be precisely and destructively ground into the shape of a wedge or a prism. Second, variations in the optical activity can occur between materials composed of the same compounds but manufactured by different freezing techniques.[6] The optical activity of the material can even vary from one growth run to another run with the same technique.[7,8] The minimum deviation method conducts refractive-index measurements for one portion of the material and then assumes that the refractive index for all of the other samples is the same as the test sample. Owing to the possibility that variations in the optical properties of a particular type of material can occur from one sample to another, making sample-specific measurements can serve as yet another factor in confirming the purity and quality of an individual sample.

Many linear and nonlinear infrared materials have different optical and nonlinear properties at room temperature and at cryogenic temperatures,[9] which presents the final challenge for the use of the minimum deviation method. It is experimentally more challenging to adapt this method to samples at cryogenic temperatures because of ambient atmospheric water condensation on the sample or other instrumentation.

In this paper we present an accurate alternative method for conducting sample-specific, nondestructive refractive-index measurements on wafer-shaped infrared materials, by rotating the sample in one arm of a Michelson interferometer. C. A. Proctor first proposed this method almost a century ago in 1907.[10] In the 1960s, M. S. Shumate provided the first experimental data using this technique using light in the visible spectrum.[11,12] Shortly thereafter, Chamberlain *et al*. adopted this method to a Mach–Zehnder

G. D. Gillen (glen.gillen@wpafb.af.mil) is with the Air Force Research Laboratory, Materials and Manufacturing Directorate/MLPJ, Anteon Corporation, Building 71A, Area B, Wright-Patterson Air Force Base, Ohio 45433. S. Guha is with the Air Force Research Laboratory, Materials and Manufacturing Directorate/MLPJ, Wright-Patterson Air Force Base, Ohio 45433.

Received 18 July 2003; revised manuscript received 5 January 2004; accepted 12 January 2004.

0003-6935/04/102054-05$15.00/0

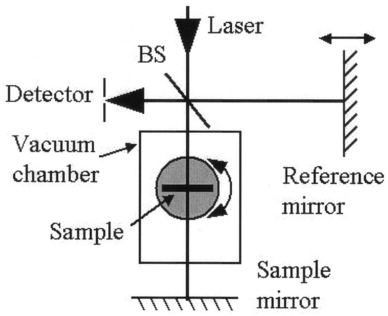

Fig. 1. Schematic of the experimental setup. The sample is mounted to the bottom of a liquid-nitrogen Dewar inside a small vacuum chamber. The sample–Dewar assembly is connected to a rotation stage outside the vacuum chamber by means of a hollow-shafted rotary feed through. BS, beam splitter.

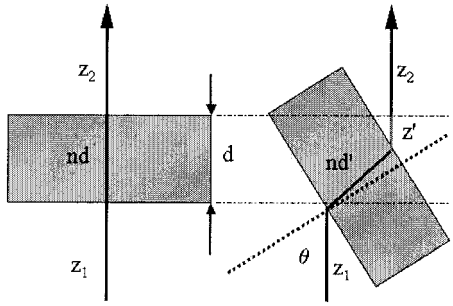

Fig. 2. Illustration of (a) a sample oriented with its normal parallel to the incident laser beam and (b) the two angle-dependent optical distances, nd' and z'.

interferometer by using a HCN maser as the light source with a wavelength of 337 μm.[13] Recently, this method has been used to measure the refractive indices of various solids[14–17] and even liquids.[18,19]

2. Experiment

$ZnGeP_2$ is a nonlinear optical material that has received a lot of attention for nonlinear processes, including frequency doubling of carbon dioxide lasers[20–23] and optical parametric oscillation.[24] In this paper we apply Proctor's method to the infrared wavelengths and measure the refractive indices of $ZnGeP_2$ for temperatures of 300 and 77 K. To the best of our knowledge, we are the first to directly measure the absolute refractive indices of $ZnGeP_2$ at 77 K.

Figure 1 shows the experimental setup utilizing a Michelson interferometer and a precision rotation stage. The laser source used is a chopped, continuous-wave, grating-tuned CO_2 laser from Access Laser Company. The measured output power at 10.611 μm is ~400 mW, and the laser beam is polarized in the horizontal direction. The sample is mounted on a rotation stage (Newport general-purpose interface bus-controlled Model 495 ACC) with a rotational resolution of 0.001°. The sample is rotated about the vertical axis, with the plane of incidence horizontal. A small area of the interference pattern is collected by using a pinhole (200-μm diameter), and the partial pattern intensity is recorded as a function of the incident angle.

The time-independent electric field of the laser before the beam splitter as a function of the optical axis, z, can be written as

$$\mathbf{E}(z_0) = A_0 \exp(ikz_0)\hat{x}, \tag{1}$$

where A_0 is the initial amplitude, k is the complex wave number, z_0 is the position of the beam splitter, and $\hat{x}$ is the direction of polarization. Using Eq. (1), and letting $z_0 = 0$, the electric field at the detector from the reference arm beam is

$$\mathbf{E}_r(z_D) = A_r \exp(i\phi_r)\hat{x}, \tag{2}$$

where the amplitude, A_r, is a function of the reflection coefficient of the beam splitter, R_{bs}, or

$$A_r = A_0\sqrt{R_{bs}(1 - R_{bs})}\,. \tag{3}$$

This is assuming that the refractive index of the beam splitter is purely real; i.e., the material is nonabsorptive. The phase of the reference arm at the detector, ϕ_r in Eq. (2), is

$$\phi_r = \frac{2\pi}{\lambda}(2z_{rm} + z_{od}), \tag{4}$$

where z_{rm} is the distance between the beam splitter and the reference arm mirror, and z_{od} is the distance between the beam splitter and the detector.

As the sample is placed in one arm of the interferometer and rotated, two changes in the optical path occur for each pass through that arm as illustrated in Fig. 2. For a sample that is oriented such that the normal to the surface is parallel to the incident laser path, the optical distance between the beam splitter and the sample mirror is $z_1 + nd + z_2$. If the sample is oriented at some other angle, θ, as illustrated in Fig. 2 then the optical path per pass is $z_1 + (nd' + z') + z_2$, where nd' is the new optical distance through the sample and z' is the additional distance traveled through the air. The optical path $(nd' + z')$ can be found to be

$$d\lfloor\sqrt{n^2 - \sin^2\theta} + 1 - \cos\theta\rfloor, \tag{5}$$

while the angle-independent phase terms for the rest of the optical path of the sample beam to the detector can be lumped together as a constant, ϕ_s. Therefore the electric field at the detector due to the sample arm has the form

$$\mathbf{E}_s(z_D) = A_s \exp\left[\frac{4\pi i d}{\lambda}(\sqrt{n^2 - \sin^2\theta} + 1 - \cos\theta) + i\phi_s\right]\hat{x}, \tag{6}$$

where

$$A_s = A_r(1 - R_s)^2, \tag{7}$$

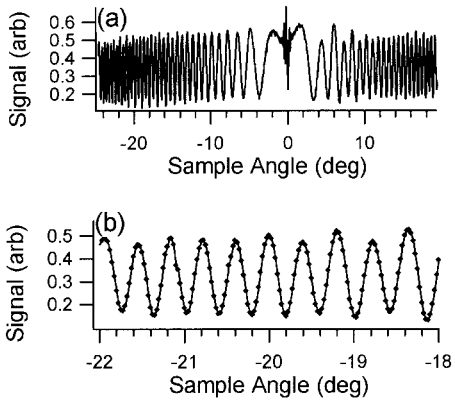

Fig. 3. (a) Recorded interferogram for a $ZnGeP_2$ sample with the laser polarization aligned with n_e and (b) a close-up of the recorded points for large angles.

if the sample is nonabsorptive and

$$A_s = A_r(1 - R_s)^2 \exp\left[-\frac{4\pi\chi d}{\lambda}\right] \tag{8}$$

if the refractive index of the sample is complex.

Superposing the fields of the sample arm and the reference arm at the detector will result in a total intensity at the detector of

$$I_D = A_r^2 + A_s^2 + 2A_rA_s \cos\left[\frac{4\pi d}{\lambda}(\sqrt{n^2 - \sin^2\theta} + 1 - \cos\theta) + \phi_0\right], \tag{9}$$

where A_r and A_s are the amplitudes of the electric fields of the reference beam and the sample beam, respectively, and ϕ_0 is the relative phase offset for $\theta = 0°$. For this model the angular variation of R_s (or the angle dependence of the surface reflectivities) is considered to be negligible over small, $\pi/8$ or less, rotations of the sample. If the angular dependence of R_s were included, it would manifest itself only as an amplitude variation of A_s and would not affect the angular position of the observed fringes.

For measurements at cryogenic temperatures the sample is held in a mount in thermal contact with the bottom of a liquid-nitrogen Dewar. To prevent room moisture from condensing and freezing on the surfaces of the sample, the entire sample mount and liquid-nitrogen cell assembly is housed inside a small vacuum chamber. The sample–liquid-nitrogen assembly is rotated by the rotation stage outside the vacuum chamber by means of a hollow-shafted rotation feed through.

The fractional portion of the interference pattern observed through the pinhole aperture as a function of the sample angle is displayed in Fig. 3, an interferogram observed for a $ZnGeP_2$ sample with a thickness of 2.906 mm. The interference pattern is recorded as the sample is rotated from a negative angle, through zero, to a set positive angle. As the sample rotates through an angle of zero, where the sample face is perpendicular to the incident laser beam, an additional interference pattern is observed, which is a result of the reflection off the front surface of the sample, acting as another arm in the interferometer. The central portion of the interferogram is thus ignored in the data analysis. The maxima and minima observed in Fig. 3 as a function of the sample angle are a result of the change in optical distance between the two arms in the interferometer. The angular position of each maximum and minimum is extracted from the data and fitted to

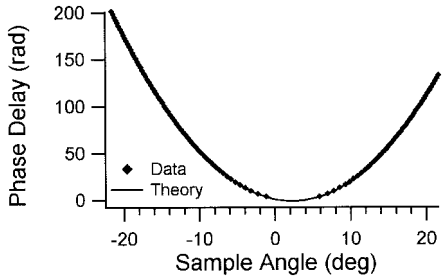

Fig. 4. Experimental and calculated angular phase delay for the interferogram of Fig. 3 as a function of the incident angle, θ.

$$m(\theta)\pi = \frac{4\pi d}{\lambda}(\sqrt{n^2 - \sin^2(\theta - \theta_0)} - \cos(\theta - \theta_0) + 1) + \phi_0. \tag{10}$$

The values assigned to $m(\theta)$ are even and odd integers for maxima and minima, respectively. The variables extracted from the numerical fit are n, θ_0, and ϕ_0. Figure 4 shows the data points and calculated fit for the interferogram observed in Fig. 3.

The fit parameters θ_0 and ϕ_0 act as horizontal and vertical shifts, respectively, for the calculated fit, while n determines the degree of vertical bend. The parameter θ_0 accounts for any slight discrepancy of the rotation stage origin with respect to normal incidence of the laser path. The parameter ϕ_0 is the fractional fringe value at normal incidence due to the difference in optical paths between the sample arm and the reference arm of the interferometer for an angle of $\theta = 0°$ and will vary from 0 to π if the observed intensity is a maximum or a minimum, respectively. Typical χ^2 values for the calculated fits are of the order of 10^{-12}. The largest contributor to the uncertainty of the measurements is that of the thickness of the sample. The sample thickness is measured by use of a high-precision micrometer with a resolution of ± 1 μm, which is comparable with the degree of uniform parallelism found for many of the samples studied. This leads to fractional uncertainties in d of approximately 10^{-3} or less for millimeter-sized samples. Uncertainties in the angular measurement for each point range from 10^{-4} to 10^{-5}, while the uncertainty of λ is of the order of 10^{-5}.

Measurements of the refractive indices of elemental semiconductors silicon and germanium were conducted as a calibration of the system first. For a slightly larger range in measured refractive-index

Table 1. Refractive-Index Measurements for Ge, Si, and $ZnGeP_2$, and Their Uncertainties[a]

Sample	n, Measured	Temp. (K)	Accepted Value	Ref.
Ge	4.003 ± 0.002	300	4.0038 at 10.5 μm	25
Si	3.428 ± 0.007	300	3.4215 at 10.0 μm	26
ZnSe	2.401 ± 0.003	300	2.4034 at 10.6 μm	27
$ZnGeP_2$	$n_o = 3.079 \pm 0.003$	300	3.0738 at 10.5 μm	28
	$n_e = 3.108 \pm 0.005$	300	3.1137 at 10.5 μm	28
$ZnGeP_2$	$n_o = 3.055 \pm 0.004$	77		
	$n_e = 3.082 \pm 0.006$	77		

[a]All measurements are for a wavelength of 10.6 μm.

values, a ZnSe window was measured as well. The results of these measurements along with those measured for the ordinary and extraordinary axes of $ZnGeP_2$ are seen in Table 1 and are compared with their accepted values. The measurements reported are the average and standard deviation for at least 10 repeated measurements. The accepted values for all of the sample types measured fall within the third decimal uncertainties of the measurements. Although this experiment was designed to measure absolute values of refractive index, the more precise birefringence value can be determined from the data. The birefringence of $ZnGeP_2$ at 100 K predicted by Fischer and Ohmer[29] of 0.037 resides in the upper range of the uncertainty of our measurements of 0.027 ± 0.01.

3. Summary

A simple method for measuring the refractive index of thin, flat-parallel materials in the long-wave infrared regime is demonstrated here. In addition, the method has been extended for long-wave infrared measurements to be performed on cryogenic samples. To the authors' knowledge, refractive-index measurements for $ZnGeP_2$ at 77 K are reported for the first time. Although the uncertainties of this method limit refractive-index measurements to the third decimal place, it is advantageous over the minimum deviation method as it provides quick, nondestructive measurements for specific samples. Results obtained thus far agree well with their known values, allowing measurements by this technique to be another reliable aid in the nondestructive characterization and identification of long-wave infrared materials. The measurement precision can be extended to the fourth decimal place with improved resolution in the thickness measurement as well as by using samples with better flatness and parallelism. A disadvantage of this method is the requirement for a wavelength stabilized laser source and a home-built Dewar–vacuum-chamber assembly for cryogenic measurements.

References

1. M. Daimon and A. Masumura, "High-accuracy measurements of the refractive index and its temperature coefficient of calcium fluoride in a wide wavelength range from 138 to 2326 nm," Appl. Opt. **41,** 5275–5281 (2002).
2. D. E. Zelmon, E. A. Hanning, and P. G. Schunemann, "Refractive-index measurements and Sellmeier coefficients for zinc germanium phosphide from 2 to 9 μm with implications for phase matching in optical frequency-conversion devices," J. Opt. Soc. Am. B **18,** 1307–1310 (2001).
3. P. S. Hauge, "Recent developments in instrumentation in ellipsometry," Surf. Sci. **96,** 108–140 (1980).
4. Z. Huang and J. Chu, "The refractive index dispersion of $Hg_{1-x}Cd_xTe$ by infrared spectroscopic ellipsometry," Infrared Phys. **42,** 77–80 (2001).
5. P. Adamson, "Laser diagnostics of nanoscale dielectric films on absorbing substrate by differential reflectivity and ellipsometry," Opt. Laser Technol. **34,** 561–568 (2002).
6. D. W. Fischer, M. C. Ohmer, P. G. Schunemann, and T. M. Pollak, "Direct measurement of $ZnGeP_2$ birefringence from 0.66 to 12.2 μm using polarized light interference," J. Appl. Phys. **77,** 5942–5945 (1995).
7. H. J. Scheel, "Historical aspects of crystal growth technology," J. Crystal Growth **211,** 1–12 (2000).
8. P. G. Schunemann, S. D. Setzler, and T. M. Pollak, "Phase-matched crystal growth of $AgGaSe_2$ and $AgGa_{1-x}In_xSe_2$," J. Crystal Growth **211,** 257–264 (2000).
9. P. Klock, *Handbook of Infrared Optical Materials* (Marcel Dekker, New York, 1991).
10. C. A. Proctor, "Index of refraction and dispersion with the interferometer," Phys. Rev. **24,** 195–201 (1907).
11. M. S. Shumate, "An interferometric measurement of index of refraction," Engineer's Degree Thesis (California Institute of Technology, Pasadena, Calif., 1964), http://etd.caltech.edu/etd/available/etd-10302002-153247/.
12. M. S. Shumate, "Interferometric measurement of large indices of refraction," Appl. Opt. **5,** 327–331 (1966).
13. J. Chamberlain, J. Haigh, and M. J. Hine, "Phase modulation in far infrared (submillimetre-wave) interferometers: III-laser refractometry," Infrared Phys. **11,** 75–84 (1971).
14. U. Schlarb and K. Betzler, "Influence of the defect structure on the refractive indices of undoped and Mg-doped lithium niobate," Phys. Rev. B **50,** 751–757 (1994).
15. S. Follonier, Ch. Bosshard, U. Meier, G. Knöpfle, C. Serbutoviez, F. Pan, and P. Günter, "New nonlinear-optical organic crystal: 4-dimethyl-aminobenzaldehyde-4-nitrophenyl-lydrazone," J. Opt. Soc. Am. B **14,** 593–601 (1997).
16. J. F. H. Nicholls, B. Henderson, and B. H. T. Chai, "Accurate determination of the indices of refraction of nonlinear optical crystals," Appl. Opt. **36,** 8587–8594 (1997).
17. M. S. Wong, F. Pan, M. Bösch, R. Spreiter, C. Bosshard, P. Günter, and V. Gramlich, "Novel electro-optic molecular cocrystals with ideal chromophoric orientation and large second-order optical nonlinearities," J. Opt. Soc. Am. B **15,** 426–431 (1998).
18. R. E. Gagnon, P. H. Gammon, H. Kiefte, and M. J. Clouter, "Determination of the refractive index of liquid carbon monoxide," Appl. Opt. **18,** 1237–1239 (1979).
19. M. Musso, R. Aschauer, A. Asenbaum, C. Vasi, and E. Wilhelm, "Interferometric determination of the refractive index of liquid sulphur dioxide," Meas. Sci. Technol. **11,** 1714–1720 (2000).
20. G. C. Bhar, S. Das, U. Chatterjee, and K. L. Vodopyanov, "Temperature-tunable second-harmonic generation in zinc germanium phosphide," Appl. Phys. Lett. **54,** 313–314 (1989).
21. A. A. Barykin, S. V. Davidov, V. D. Dorokhov, V. P. Zakharov, and V. V. Butuzov, "Generation of the second harmonic of CO_2 laser pulses in a $ZnGeP_2$ crystal," Quantum Electron. **23,** 688–693 (1993).
22. H. M. Hobgood, T. Henningsen, R. N. Thomas, R. H. Hopkins, M. C. Ohmer, W. C. Mitchel, D. W. Fischer, S. M. Hedge, and

F. K. Hopkins, "$ZnGeP_2$ grown by the liquid encapsulated Czochralski method," J. Appl. Phys. **73,** 4030–4037 (1993).
23. P. D. Mason, D. J. Jackson, and E. K. Gorton, "CO_2 laser frequency doubling in $ZnGeP_2$," Opt. Commun. **110,** 163–166 (1994).
24. K. L. Vodopyanov and P. G. Schunemann, "Broadly tunable noncritically phase-matched $ZnGeP_2$ optical parametric oscillator with a 2-μJ pump threshold," Opt. Lett. **28,** 441–443 (2003).
25. E. D. Palik, "Germanium (Ge)," in *Handbook of Optical Constants of Solids* (Academic, New York, 1998), pp. 471–478.
26. E. D. Palik, "Silicone (Si)," in *Handbook of Optical Constants of Solids* (Academic, New York, 1998), pp. 555–568.
27. E. D. Palik, "Zinc Selenide (ZnSe), Zinc Telluride (ZnTe)," in *Handbook of Optical Constants II* (Academic, New York, 1991), pp. 751–758.
28. G. D. Boyd, E. Buehler, and F. G. Storz, "Linear and nonlinear optical properties of $ZnGeP_2$ and CdSe," Appl. Phys. Lett. **18,** 301–304 (1971).
29. D. W. Fischer and Mc C. Ohmer, "Temperature dependence of $ZnGeP_2$ birefringence using polarized light interference," J. Appl. Phys. **81,** 425–431 (1997).